

DOI: <https://dx.doi.org/10.21123/bsj.2023.7708>

Ni²⁺, Pt⁴⁺, Pd²⁺, and Mn²⁺ Metal ions Complexes with Azo Derived from Quinolin-2-ol and 3-amino-N-(5-methylisoxazol-3-yl) Benzenesulfonamide: Synthesis, Characterization, Thermal Study, and Antioxidant Activity

Adhraa Ghazi Abdulrazzaq^{1*} 

Abbas Ali Salih Al-Hamdani² 

¹AL-Israa-University-College, Department of Medical Instrumentation, Baghdad, Iraq.

²Department of Chemistry, College of Science for Women, University of Baghdad, Iraq.

*Corresponding author: azraa.ghazi1105a@csu.uobaghdad.edu.iq

E-mail address: abbasas_chem@csu.uobaghdad.edu.iq

Received 9/9/2022, Revised 28/11/2022, Accepted 30/11/2022, Published Online First 20/4/2023,
Published 01/12/2023



This work is licensed under a [Creative Commons Attribution 4.0 International License](https://creativecommons.org/licenses/by/4.0/).

Abstract:

Diazotization reaction between quinolin-2-ol and (2-chloro-1-(4-(N-(5-methylisoxazol-3-yl)sulfamoyl)phenyl)-2-iazyn-1-ium was carried out resulting in ligand-HL, this in turn reacted with the next metal ions (Ni²⁺, Pt⁴⁺, Pd²⁺, and Mn²⁺) forming stable complexes with unique geometries such as (tetrahedral for both Ni²⁺ and Mn²⁺, octahedral for Pt⁴⁺ and square planer for Pd²⁺). The creation of such complexes was detected by employing spectroscopic means involving ultraviolet-visible which proved the obtained geometries, fourier transfer proved the formation of azo group and the coordination with metal ion through it. Pyrolysis (TGA & DSC) studies proved the coordination of water residues with metal ions inside the coordination sphere as well as chlorine atoms. Moreover, element micro-analysis and AAS that gave corresponding outcome with theoretically counting outcome. (¹H & ¹³C-NMR) and magnetic quantifications can also indicate the formation of ligand-HL and occurrence of coordination. Antioxidant activities of these compounds were evaluated against (DPPH) radical and were compared to the standard natural antioxidant, ascorbic acid. The findings showed that these compounds exhibit excellent radical scavenging activities

Keywords: Antioxidant, Azo dye, Mass spectroscopy, Sulfamethoxazole, Thermal analysis.

Introduction:

Azo dyes derived from aromatic amines and their mineral complexes are characterized by applicability in multi usages. Furthermore, such compounds have special interest in many researches, this contributes to their applications as textile dyes, pharmaceutical materials and indicators. ¹ Azo-dyes have biological activities such as antibacterial, antifungal, anti-HIV and antitumor, so they have immense importance in medicinal chemistry. ² Furthermore, they have important roles in food and analytical chemistry.³ Among these compounds, heterocyclic azo-dyes and their metal complexes can be involved in biological reactions like nitrogen fixation and RNA inhibition, in cosmetics as well as in non-linear optics protein synthesis. ^{4,5} Sulfa compounds are well known as useful antibiotics in the assorted microbial contagion treatment ⁶⁻⁸ Nevertheless, the high applications of these compounds stimulate

allergic side effects to many body organs ^{9, 10} as well as lymphadenopathy, hepatotoxicity, and haematological disorders ¹¹. In order to beat such quandaries and to make efficient drugs, new functionalized sulfonamide derivatives and their transition metal complexes ¹²⁻¹⁵ were employed in clinical trials. Metal sulfonamide complexes were more effective than the drugs from which they come. Also, the azo dyes have been testified to display diversity in bio-vitality, involving anti-inflammatory, antibacterial, and antiviral ¹⁵ activities. Sulfamethoxazole (SMX), a sulfonamide drug has a structural analogue of p-aminobenzoic acid that inhibits the synthesis of intermediary dihydro folic acid from its precursors. It is a bacteriostatic antibiotic, used in synergistic combination therapy with Trimethoprim for the treatment of urinary tract infections, respiratory tract pathogens, skin pathogens, certain enteric

pathogens; and as a substitute to amoxicillin-based antibiotics in treating sinusitis and prophylaxis of pneumonia in patients living with AIDS. The clinical importance of sulfamethoxazole and trimethoprim-sulfamethoxazole combination has slowly declined in the most recent decades, largely as a result of the development and rapid spread of resistance to these agents among all major bacterial pathogens¹⁶. Moreover, for this reason, we aimed to prepare a new class of sulfamethaxazole-based drugs, by making a chemical combination with 2-hydroxy quinolone (quinolin-2-ol). Then investigate the formation of such combination using spectroscopic methods, then allowing this azo-ligand to react with a series of metal salts including (Pt^{4+} , Pd^{2+} , Ni^{2+} and Mn^{2+}), then investigating the formation of the complexes using the same methods that used with ligand.

Chemicals and Method:

1. Materials and Instrumentation

Materials have been obtained from the trading suppliers, (SigmaAldrich, Merck, and others). The eurovectormodel EA/3000, singleV30, has been employed to achieve (C-H-N-SandO). Mineral-ions have determined as M-O employing a gravimitrec-approaches. Molar conductivity has been estimated employing Conduct meter W-T-W, 25-°C. 1×10^{-3} M. D/M/S/O has been employed as solvent. Mas.s-spectra for substances have been collected using mas.s spectrometry (MS) Q-P-50-A-D-I Analysis Shimadzu QP(E170Ev) -2010-Pluss spectrometer. The spectra were analyzed using a Shimadzu UV-1800 UV-visible spectrophotometer. The photonuclear magnetic resonance (^1H & ^{13}C -NMR) spectra for ligand in DMSO- d_6 were recorded using a Bruker 400 MHz. The IR Prestige-21 was used to investigate the Fourier transform infrared (FTIR) spectra (ranges between 4000-600 cm^{-1}).

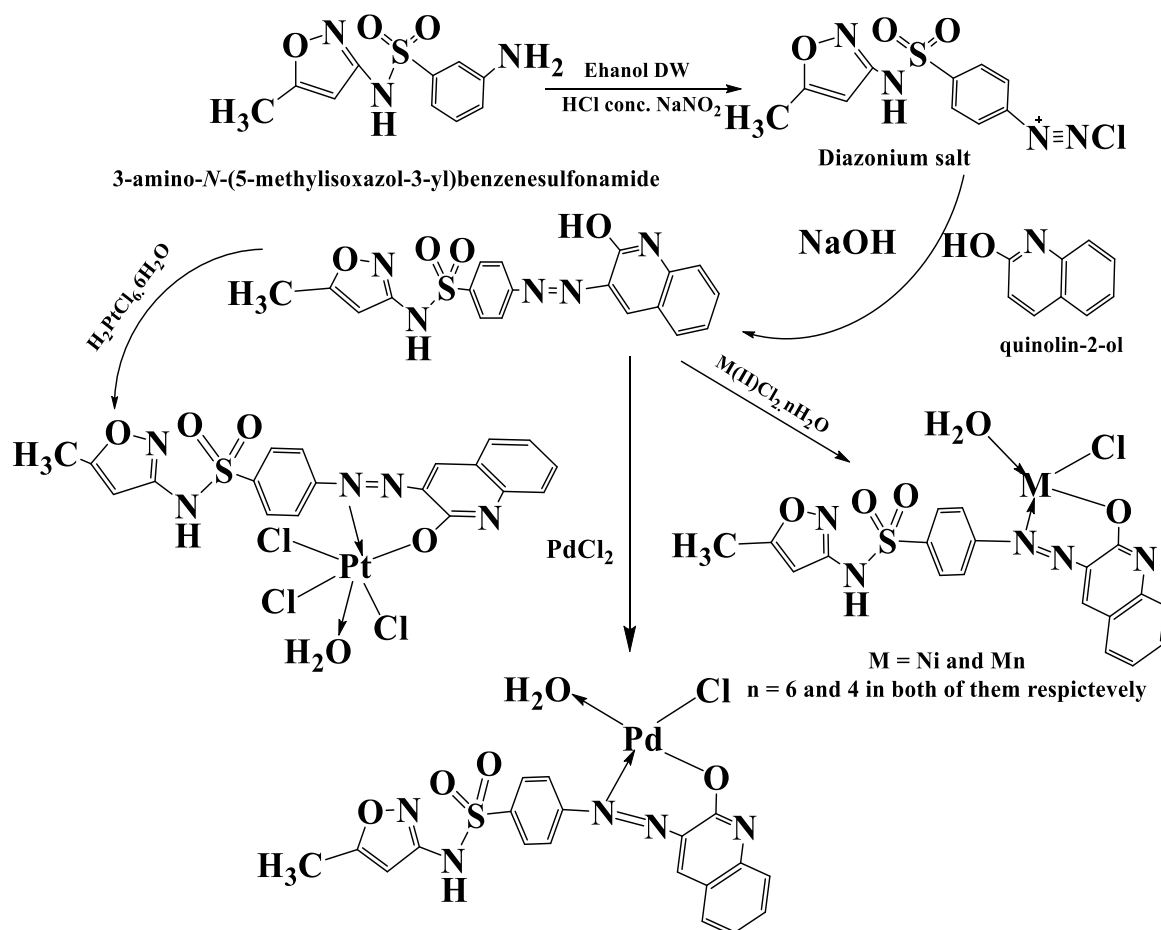
2. Synthesis of Azo Dye Ligand

The ligand in Scheme 1 was synthesized according to the suggested method at which an

amount of (2.05 g, 0.005 mol)¹⁷ from Sulfamethoxazole (3-amino-N-(5-methylisoxazol-3-yl)benzenesulfonamide) is dissolved in a mixture consisting of 4 mL of 37% HCl and 35 mL distilled water DW. Then this mixture is allowed to be cooled in a temperature starts at 0°C up to 5°C followed by discontinuously addition of (0.375 g, 0.005 mol) NaNO_2 solution which in turn is dissolved in 30 mL DW, with continuous stirring and under controlling the range of temperature, which must be kept around 5°C for 30 minutes. After 15 minutes, diazotization-coupling operation occurs resulting in diazonium salt, which in turn added through filtered funnel containing cube of ice of DW onto 0.726 g, 0.005 mol solution of 2-hydroxy quinolin (quinolin-2-ol) dissolved in 50ml of absolute EtOH and 15 ml of 10% NaOH solution with cooling and continuous stirring. We can clearly observe the creation of reddish-brown precipitate scheme 1, this precipitate is left for one hour under 5 °C, then filtered and washed several periods with distilled water. Finally, recrystallization process by absolute ethanol is carried out, followed by drying in oven at 50 °C. yielding in 68% product having (133-135) °C m. p.

3. General Approach for Metal Complexes Synthesis

A specific amount of azo-ligand, which dissolved in absolute ethanol, is added discontinuously with continuous stirring onto a specific amount for each of the next metal salts: (Pt^{4+} , Pd^{2+} , Ni^{2+} and Mn^{2+}) solutions. The resultant mixture is heated and refluxed for one hour up to 80 °C, followed by cooling at room temperature. After 24 hours, a completely precipitation occurs, scheme 1. Then, solution containing- precipitate is filtered, washed several times with distilled water and washed with little amount of cold ethanol. Finally, recrystallization process using absolute ethanol is carried out for the synthesized complexes. The molar ratio of the synthesized complexes has been found to be 1:1 M: L.



Result and Discussion:

1. Physical and Chemical Properties

Reactions of metal salts with ligand gave the synthetic complexes (Scheme 1). The results of

elemental analysis demonstrates 1:1 M:L stoichiometry for all complexes. The elemental analysis results were compatible with theoretical calculated results as denoted in Table 1.

Table 1. Some physical properties element micro analysis studies of ligand and complexes

Compound M _w	m-p _c	Color	Eleme. Micro-ana. percentage estm. (calc.)						
			C	H.	N.	O.	S	M.	Cl.
C ₁₉ H ₁₅ N ₅ O ₄ S 409.42	130-133	Pale brown	55.50 (54.41)	3.62 (3.18)	17.10 (18.70)	15.55 (15.26)	7.39 (8.40)	--	--
C ₁₉ H ₁₆ N ₅ NiO ₅ SCl 520.57	264 d	Pale brown	44.33 (43.84)	3.39 (3.10)	14.41 (13.45)	14.83 (15.37)	5.61 (6.16)	12.07 (11.27)	5.98 (6.81)
C ₁₉ H ₁₆ N ₅ PdO ₅ SCl 568.30	214 d	Dark brown	41.14 (40.16)	1.93 (2.84)	13.30 (12.32)	13.39 (14.08)	5.98 (5.64)	17.79 (18.73)	7.07 (6.24)
C ₁₉ H ₁₆ ClMnN ₅ O ₅ S 516.82	234 d	Brown	44.15 (43.38)	3.04 (2.65)	13.60 (14.68)	15.40 (14.40)	6.26 (7.27)	10.70 (11.20)	6.93 (6.95)
C ₁₉ H ₁₆ N ₅ PtO ₅ SCl ₃ 727.86	220 d	Dark brown	12.76 (13.35)	1.96 (2.22)	10.66 (9.62)	11.73 (10.99)	3.77 (4.41)	27.72 (26.80)	15.51 (14.61)

d= decompose

2. Magnetic Nuclear Resonance Spectrum of Ligand (¹H-NMR & ¹³C-NMR)

Magnetic nuclear resonance spectrum of the new azo ligand was studied using dimethyl sulfoxide DMSO-d₆ as solvent and TMS as standard reference. Fig. 1 demonstrates the chemical shifts of these spectra. ¹H-NMR spectrum of the ligand

demonstrates several chemical shifts, those as follows: singlet signals: 1H of Ar-OH group, 1H of N-H amino group, 2H of both (aromatic C-H which nearby to CH₃ and 3-quinoline of C-H group which nearby to OH), and 3H of CH₃ group these signals were observed at : 1.08 ppm, 10.51 ppm, (6.72-6.79) ppm and 2.60 ppm respectively. We also

observed only one multiplet signal at (7.68-7.95) ppm attributed to 8H of Ar-H in addition to solvents signal (DMSO) which observed at (2.41-2.51) ppm. ^{13}C -NMR spectrum in Fig. 1 demonstrates the next signals : (100.622 MHz, DMSO- d_6): d 48.06 (C1),

167.70 (C13), 144.31 (C7), 121.95 (C18), 148.76 (C19), 125.18 (C15), 130.31 (C17), 134.31 (C9), 141.97 (C8), 115.39 (C16), 167.70 (C13), 151.10 (C11), 153.24 (C5), 195.60 (C12), 131.97 (C14), 162.15 (C4), 157.17 (C10), 179.82 (C2) ^{18,19}

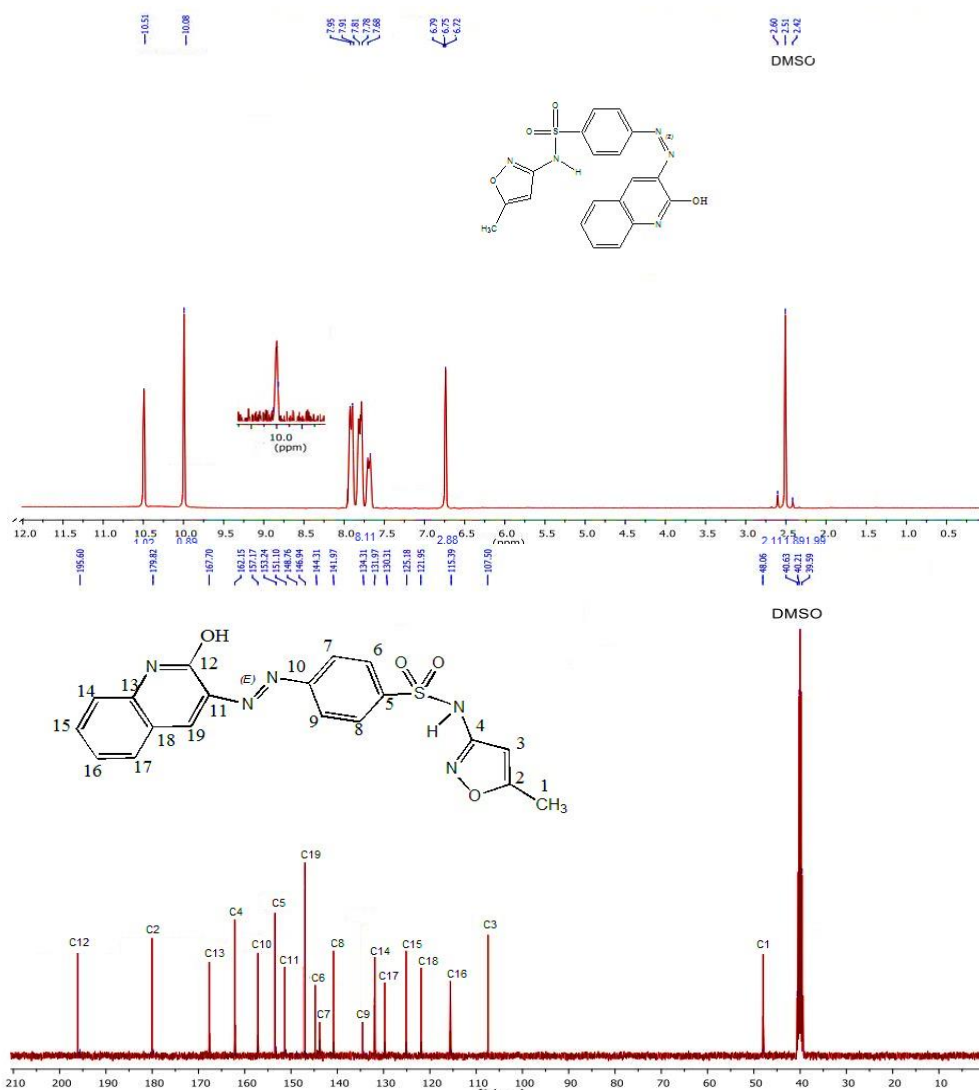


Figure 1. ^1H & ^{13}C -NMR spectra of ligand (HL)

3. UV-Vis Studies of the Ligand (HL) and Its Complexes:

Figure 2 and Table 2 illustrate the electronic transitions of the ligand at ultra violet region in the range 296 nm, 33783 cm^{-1} and 328 nm, 30487 cm^{-1} those absorption bands belong to ($\pi \rightarrow \pi^*$) and ($n \rightarrow \pi^*$) electronic transitions respectively. The presence of non-bonding electrons or heteroatoms causes ($n \rightarrow \pi^*$) transition, while the presence of unsaturated bonds and aromatic rings causes ($\pi \rightarrow \pi^*$) transition ²⁰. We can apparently observe in Fig. 3, the occurrence of coordination in $[\text{Mn}(\text{L})\text{Cl}(\text{H}_2\text{O})_2]$, is because of the observed shifting in absorption range of detected transitions at ultra violet region compared to the range of the same transitions in free (HL) to appear at 296 nm,

33783 cm^{-1} and 322 nm, 31055 cm^{-1} . Other indication supports the coordination is clear of the d-d transitions in the metal itself, those transitions denoted as $^6\text{A}_1 \rightarrow ^4\text{T}_{1(\text{G})}$ at (493 nm, 20283 cm^{-1}) and $^6\text{A}_1 \rightarrow ^4\text{T}_{2(\text{G})}$ at (703 nm, 14224 cm^{-1}) and the magnetic moment (3.71 B.M) can definitely support tetrahedral geometry ^{21,22}. Figure 4 of $[\text{Pd}(\text{L})(\text{H}_2\text{O})\text{Cl}]$ complex shows electronic transitions in ultra violet region resemble those in ligand in its free form with some modifications including shifting and intensity changes because of the coordination with metal ion, those are ($\pi \rightarrow \pi^*$) and ($n \rightarrow \pi^*$)+(C.T) at 298 nm, 33557 cm^{-1} and 339 nm, 29498 cm^{-1} respectively. Additionally, $^1\text{A}_1\text{g} \rightarrow ^1\text{B}_1\text{g}$ and $^1\text{A}_1\text{g} \rightarrow ^1\text{A}_2\text{g}$ (d-d transitions) can clearly be observed at 582 nm, 17182 cm^{-1} and

721nm, 13869 cm^{-1} respectively. Those transitions can definitely support square planer geometry ²³. [Pt(L)(H₂O)Cl] complex shows the following transitions : $\pi \rightarrow \pi^*$ at 306 nm, 32679 cm^{-1} , $n \rightarrow \pi^*$ at 333 nm, 30030 cm^{-1} and C.T(M \rightarrow L) transition at 398 nm, 25125 cm^{-1} those belong to ligand with some shifting that supports the coordination. Other transitions are (d-d) transitions that referred to as

$^1A_{1g} \rightarrow ^1T_{2g}$ at 659 nm, 15174 cm^{-1} and $^1A_{1g} \rightarrow ^1T_{1g}$ at 768 nm, 13020 cm^{-1} ; the mentioned transitions can definitely support octahedral geometry of the complex ²³. All the electronic transitions information for the ligand (HL) & products are displayed in Table 2 in addition to the information of [Ni(L)Cl(H₂O)] complex and other complexes ²³.

Table 2. UV-Vis spectral data of ligand L and its complexes

Compound	λ_{max} (nm)	ν cm^{-1}	ABS.	ϵ_{max} L mol ⁻¹ cm ⁻¹	Assignment	Λ_{m} cm ² mol ⁻¹	Ω	μ_{eff} B.M
C ₁₉ H ₁₅ N ₅ O ₄ S HL	296	33783	1.501	1501	$\pi \rightarrow \pi^*$	18	9	3.89
	328	30487	0.926	926	$n \rightarrow \pi^* + \text{C.T(L} \rightarrow \text{L)}$			
	296	33783	0.389	389	$\pi \rightarrow \pi^*$			
	322	31055	0.292	292	$n \rightarrow \pi^*$			
	376	26595	0.187	187	C.T			
[Mn(L)Cl(H ₂ O) ₂] Tetrahedral	493	20283	0.567	567	$^6A_{1g} \rightarrow ^4T_{1(G)}$	9	3.71	
	703	14224	0.193	193	$^6A_{1g} \rightarrow ^4T_{2(G)}$			
[Pd(L)(H ₂ O)Cl] (Square planer)	298	33557	1.964	1964	$\pi \rightarrow \pi^*$	21	12	Diamagnetic
	339	29498	2.091	2091	$n \rightarrow \pi^* + (\text{C.T})$			
	582	17182	0.489	489	$^1A_{1g} \rightarrow ^1B_{1g}$			
	721	13869	0.301	301	$^1A_{1g} \rightarrow ^1A_{2g}$			
[Ni(L)Cl(H ₂ O)] (Tetrahedral)	302	33112	0.282	282	$\pi \rightarrow \pi^*$	12	2.66	
	339	29498	0.256	256	$n \rightarrow \pi^*$			
	392	25510	0.279	279	$n \rightarrow \pi^* + (\text{C.T})$			
	648	15432	0.056	56	$^3T_{1(F)} \rightarrow ^3T_{1(F)}$			
	797	12547	0.022	22	$^3T_{1(F)} \rightarrow ^3A_2$			
[Pt(L)(H ₂ O)Cl] (Octahedral)	821	12180	0.021	21	$^3T_{1(F)} \rightarrow ^3T_{1(P)}$	17	17	Diamagnetic
	306	32679	0.086	86	$\pi \rightarrow \pi^*$			
	333	30030	0.093	93	$n \rightarrow \pi^*$			
	398	25125	0.123	123	C.T(M \rightarrow L)			
	659	15174	0.022	22	$^1A_{1g} \rightarrow ^1T_{2g}$			
768	13020	0.026	26	$^1A_{1g} \rightarrow ^1T_{1g}$				

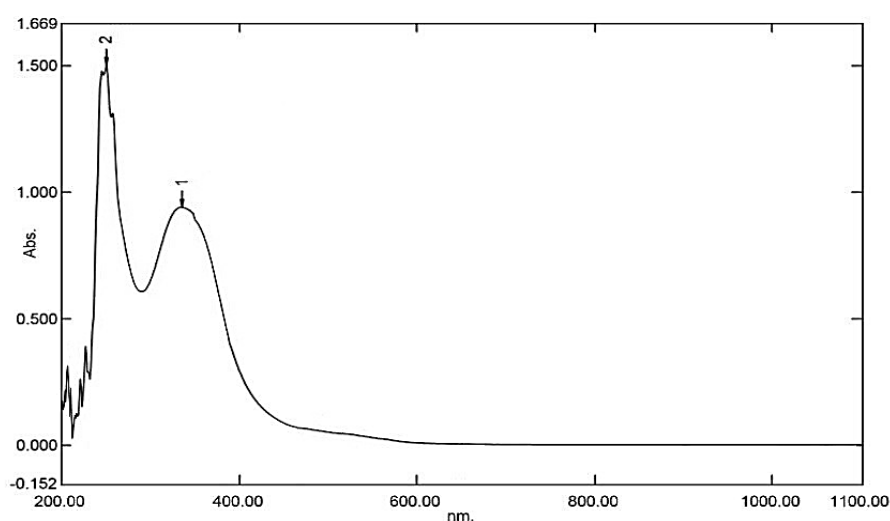


Figure 2. UV-Vis spectrum of ligand (HL)

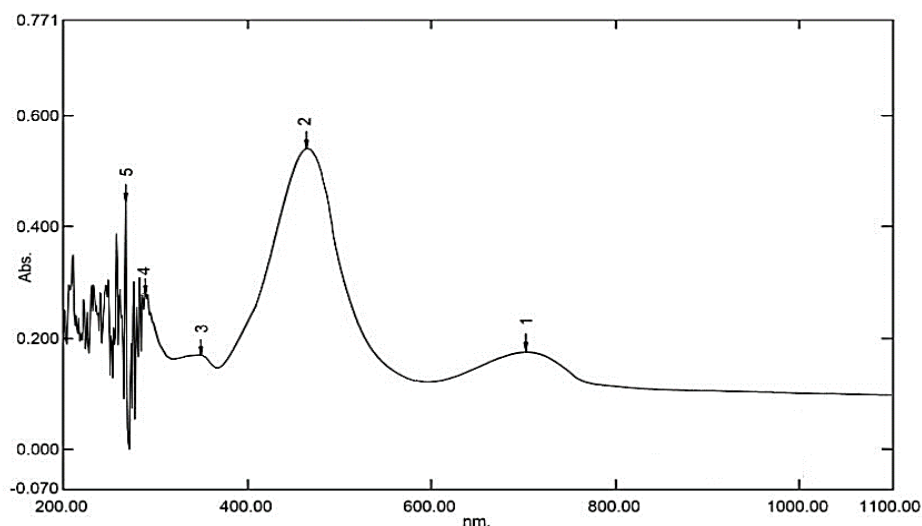


Figure 3. UV-Vis spectrum of Mn-L

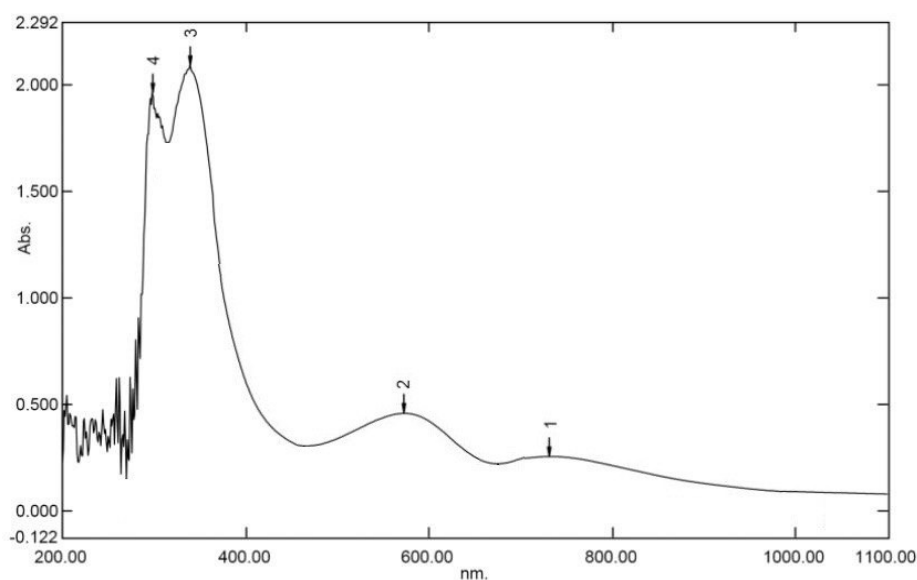


Figure 4. UV-Vis spectrum of Pd-L

4. LC-Mass Spectrum. of HL & Some Products: LC-Mass spectrum. of ligand (HL) & some products were tested using LC-Mass device, this approach is one of the most important approaches in characterization and complementary for the rest approaches by which the molecular weight of the compound is estimated according to the relation (m/z). Mass information of the ligand in Scheme 2 shows the fragmentation pattern and the extract mass for each pattern. We can clearly observe the molecular ion peak $[M]^+$ for the fragment $C_{10}H_9N_2O_3S^+$ and its relative abundance about 45% in Fig. 5, in addition to other abundances for the rest of peaks including $C_9H_6N_3O^+$, $C_6H_6NO_2S^+$, $C_7H_7^+$, $C_2H_6N_3O^+$ and $C_4H_4NO^+$ mentioned in Table. 3 and corresponded the next abundances : 43% , 15% , 13% , 33% and 42% respectively ¹⁹. For $[Pt(L)(H_2O)Cl]$, Fig. 6 and Scheme 3, we can also detect the molecular ion peak (M^+) at 727 m/z with

relative abundance 20% and next patterns: $C_{19}H_{14}Cl_3PtN_5O_3S^+$, $C_9H_5PdN_2O^+$, $C_{10}H_{10}N_3O_3S^+$, $C_3H_4PdNO^+$, $C_6H_6NO_2S^+$, $C_4H_5N_2O^+$ and $C_6H_6N^+$, which corresponded to 709 m/z , 387 m/z , 265 m/z , 252 m/z , 156 m/z , 97 m/z and 92 m/z respectively ¹⁹. Additionally, $[Ni(L)Cl(H_2O)]$ complex in Fig. 7 and Scheme 4, illustrate the next fragments: (M^+) at 520 m/z with relative abundance 12%, $C_{19}H_{14}N_5NiO_4S^+$, $C_{10}H_{10}N_3O_3S^+$, $C_9H_5N_2NiO^+$, $C_6H_6NO_2S^+$, $C_3H_4NiNO^+$, $C_4H_5N_2O^+$ and $C_6H_6N^+$ that correspond to 467 m/z , 252 m/z , 215 m/z , 156 m/z , 128 m/z , 97 m/z and 92 m/z respectively ²⁴. Finally, Fig. 8 and Scheme 5 of $[Pd(L)(H_2O)Cl]$ complex illustrate the next fragments: (M^+) at 568 m/z with relative abundance 10%, $C_{19}H_{14}N_5O_4PdS^+$, $C_9H_5PdN_2O^+$, $C_{10}H_{10}N_3O_3S^+$, $C_3H_4PdNO^+$, $C_6H_6NO_2S^+$, $C_4H_5N_2O^+$ and $C_6H_6N^+$ corresponded to 514 m/z , 263 m/z , 252 m/z , 176 m/z , 156 m/z , 97 m/z and 92 m/z respectively ²⁴.

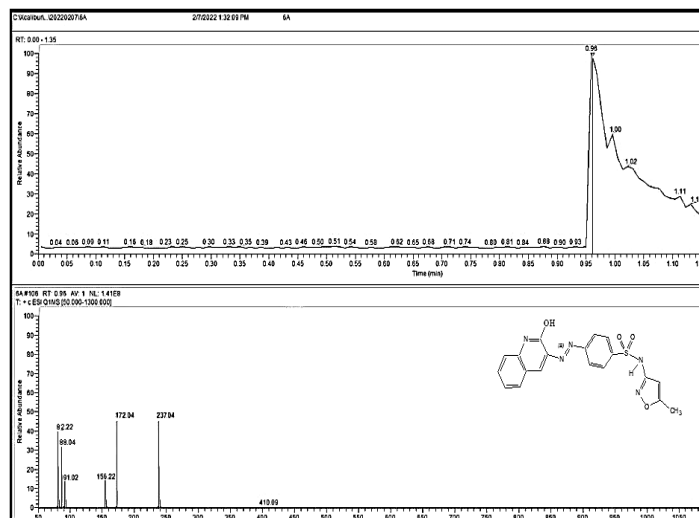


Figure 5. LC-Mass spectrum ligand (HL)

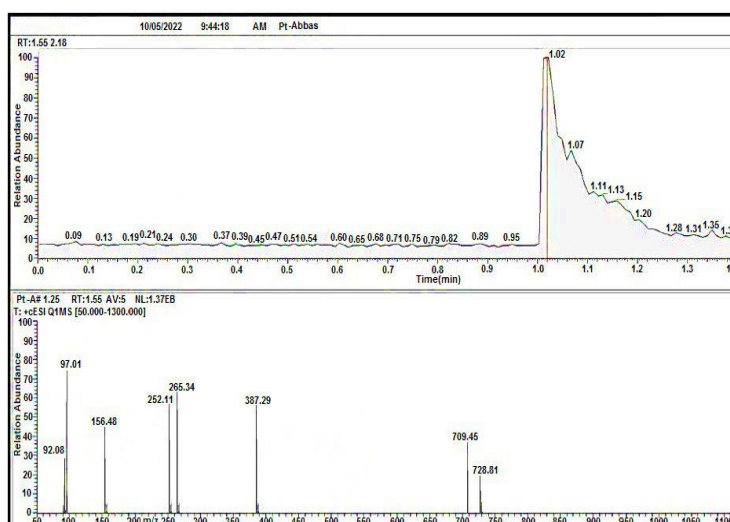


Figure 6. LC-Mass spectrum of Pt-L

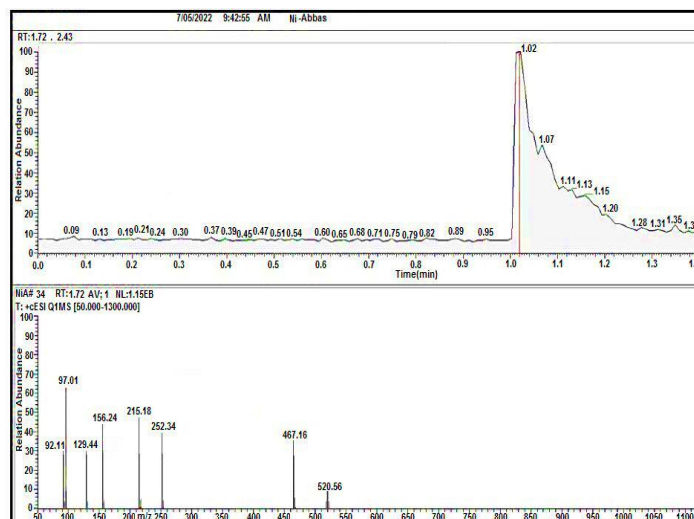


Figure 7. LC-Mass spectrum of Ni-L

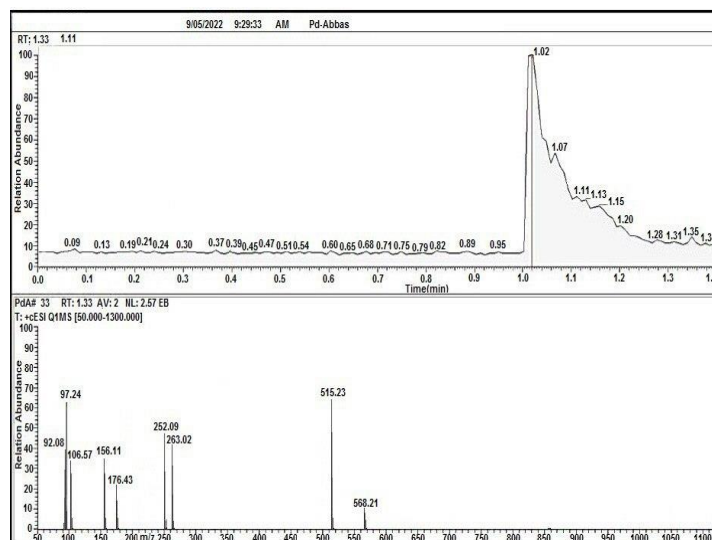
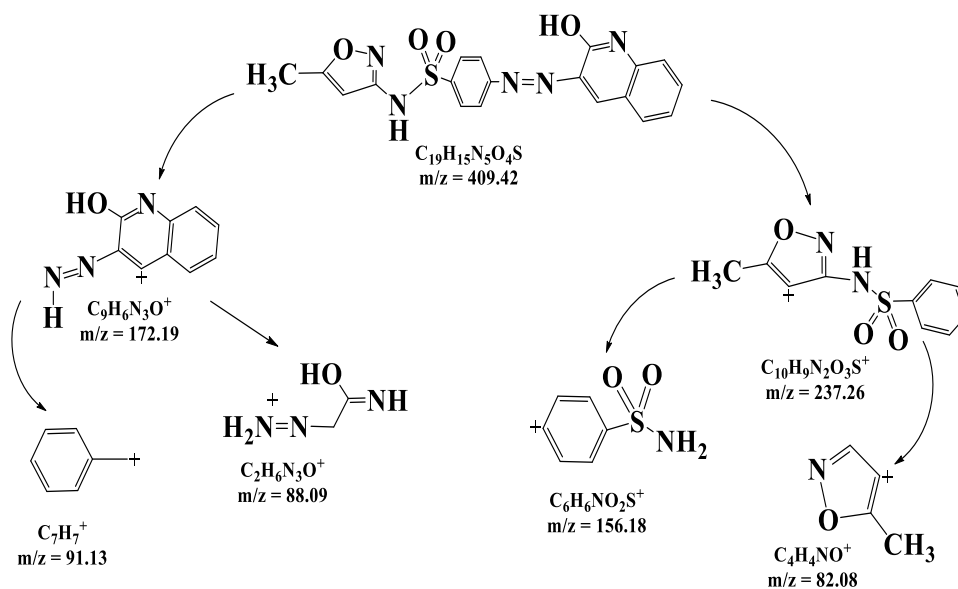
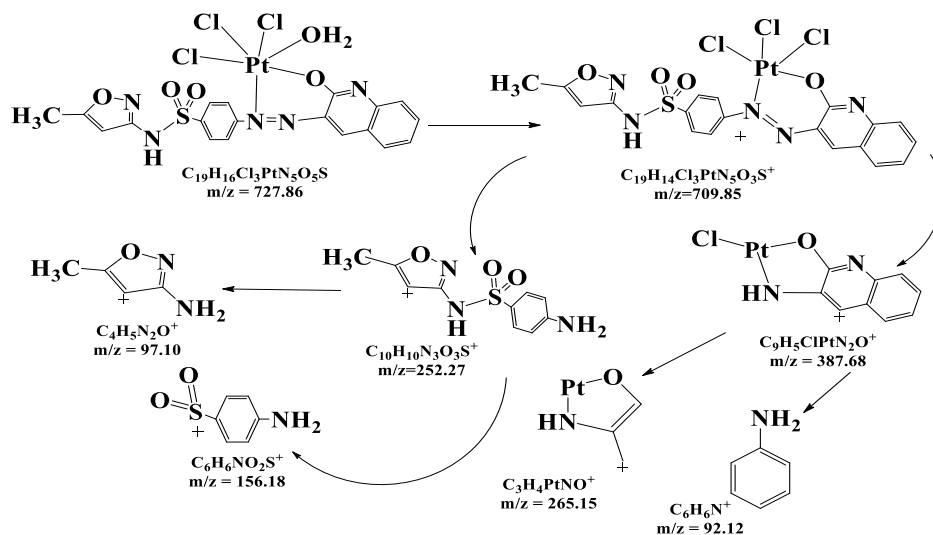


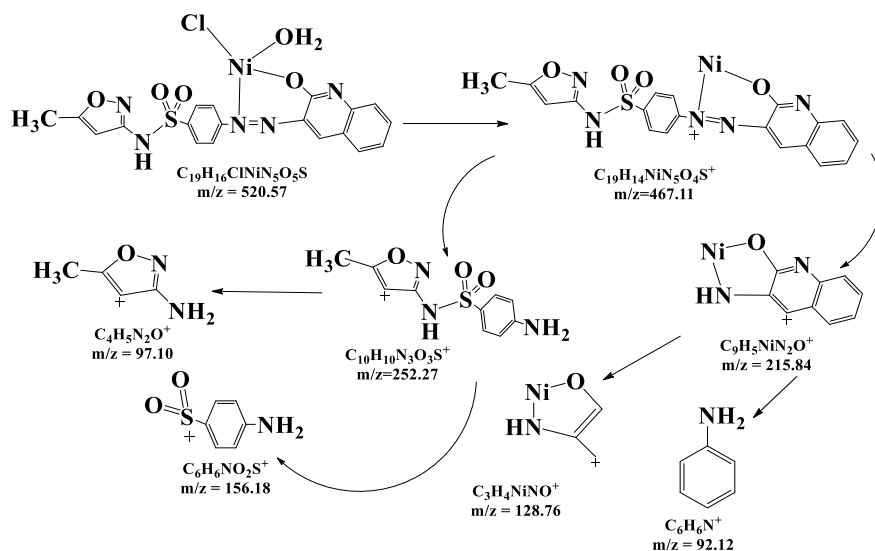
Figure 8. LC-Mass spectrum of Pd-L



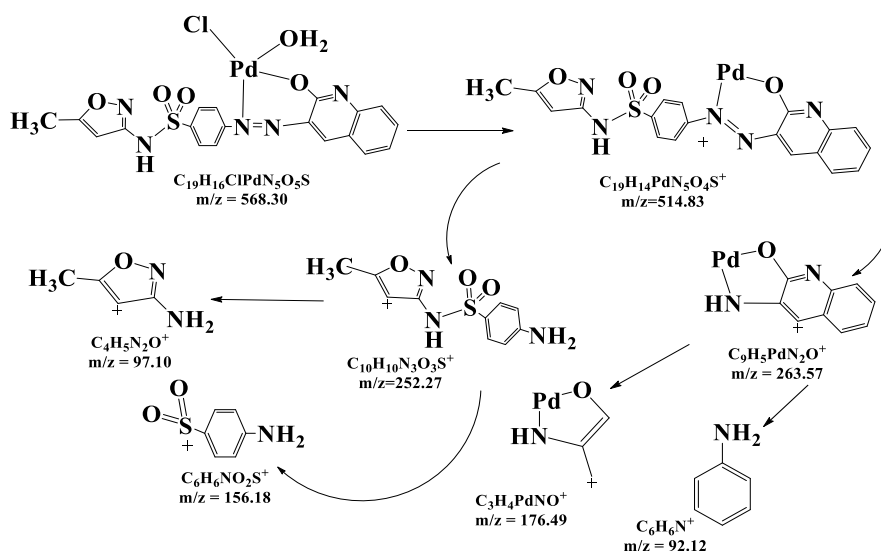
Scheme 2. Fragmentation analogues of ligand (HL)



Scheme 3. Fragmentation analogues of Pt-L



Scheme 4. Fragmentation analogues of Ni-L



Scheme 5. Fragmentation analogues of Pd-L

Table 3. LC-Mass spectral data of ligand L and its complexes

Fragment L	Extract mass	Relative abundance	Fragment Ni-complex	Extract mass	Relative abundance
C ₁₉ H ₁₅ N ₅ O ₄ S	409	2%	C ₁₉ H ₁₆ ClN ₅ NiO ₅ S	520	12%
C ₁₀ H ₉ N ₂ O ₃ S ⁺	237	45%	C ₁₉ H ₁₄ N ₅ NiO ₄ S ⁺	467	38%
C ₉ H ₆ N ₃ O ⁺	172	43%	C ₁₀ H ₁₀ N ₃ O ₃ S ⁺	252	42%
C ₆ H ₆ NO ₂ S ⁺	156	15%	C ₉ H ₅ N ₂ NiO ⁺	215	48%
C ₇ H ₇ ⁺	91	13%	C ₆ H ₆ NO ₂ S ⁺	156	45%
C ₂ H ₆ N ₃ O ⁺	88	33%	C ₃ H ₄ NiNO ⁺	128	31%
C ₄ H ₄ NO ⁺	82	42%	C ₄ H ₅ N ₂ O ⁺	97	62%
--	--	--	C ₆ H ₆ N ⁺	92	30%
Fragment Pd-complex	Extract mass	Relative abundance	Fragment Pt-complex	Extract mass	Relative abundance
C ₁₉ H ₁₆ ClN ₅ O ₅ PdS	568	10%	C ₁₉ H ₁₆ Cl ₃ N ₅ PtO ₅ S	727	20%
C ₁₉ H ₁₄ N ₅ O ₄ PdS ⁺	514	65%	C ₁₉ H ₁₄ Cl ₃ N ₅ PtO ₃ S ⁺	709	38%
C ₉ H ₅ PdN ₂ O ⁺	263	42%	C ₉ H ₅ ClN ₂ PtO ⁺	387	58%
C ₁₀ H ₁₀ N ₃ O ₃ S ⁺	252	48%	C ₃ H ₄ NPtO ⁺	265	65%
C ₃ H ₄ PdNO ⁺	176	23%	C ₁₀ H ₁₀ N ₃ O ₃ S ⁺	252	59%
C ₆ H ₆ NO ₂ S ⁺	156	36%	C ₆ H ₆ NO ₂ S ⁺	156	45%
C ₄ H ₅ N ₂ O ⁺	97	63%	C ₄ H ₅ N ₂ O ⁺	97	75%
C ₆ H ₆ N ⁺	92	40%	C ₆ H ₆ N ⁺	92	29%

5. FT-IR Studies:

FT-IR spectrum of ligand in Fig. 9, displays unique absorption band attributed to azo group formation. Synthesis of such group causes the appearance of N=N stretching absorption band in the range (1448 -1403) cm^{-1} , this band is a strong evidence which supports the formation of ligand. In addition to the disappearing of asymmetric stretching vibrational mode of NH_2 group because of diazotization coupling reaction through this group with 2-hydroxyquinolin. Other absorption bands were clearly observed at 3381 cm^{-1} , 3091 cm^{-1} , 2977 cm^{-1} and (1160 -1086) cm^{-1} for each of the following groups : (NH) amine, (C-H) aromatic, (C-

H) aliphatic and (SO_2) respectively ²⁵. For Pd-complex in Fig. 10, we can clearly notice the occurrence of coordination depending on the shifting in the ranges of absorption bands for azo-group by the range (32-13) cm^{-1} to be observed at (1480-1390) cm^{-1} ²⁶. For Mn-complex, the absorption of azo band was shifted by 60 cm^{-1} compared to free ligand to be observed at 1388 cm^{-1} ²⁷ and Ni-complex by the range (21-34) cm^{-1} and observed at (1469-1369) cm^{-1} ²⁸. This can strongly proves the occurrence of coordination. Table 4 demonstrates all FT-IR spectral data of the ligand and some of its complexes.

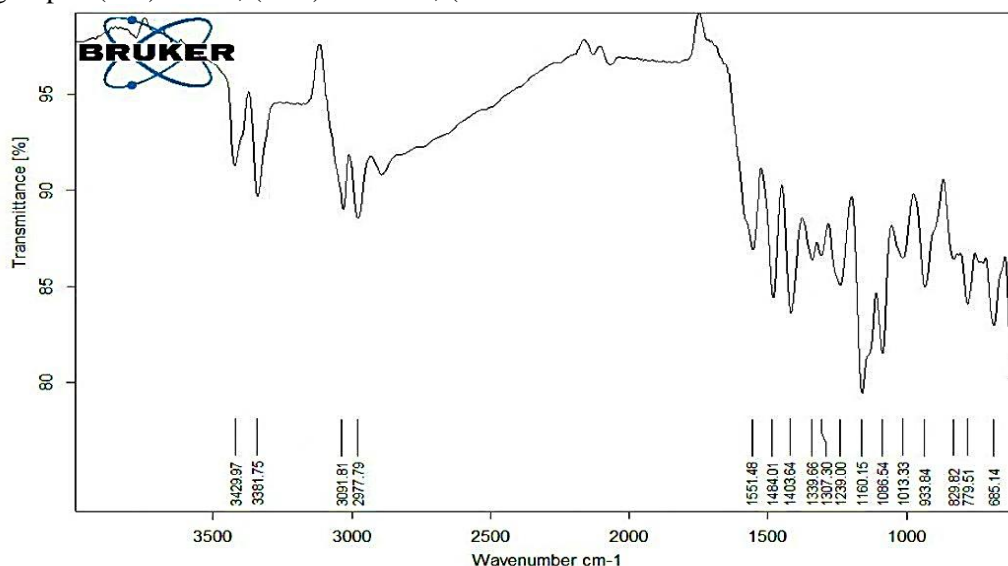


Figure 9. FT-IR spectrum of ligand (HL)

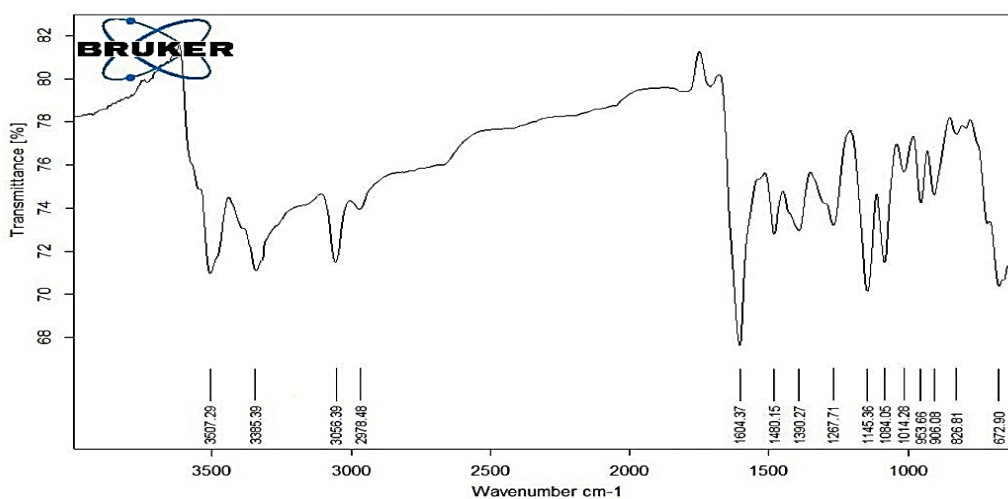


Figure 10 (a) . FT-IR spectrum of Pd-L

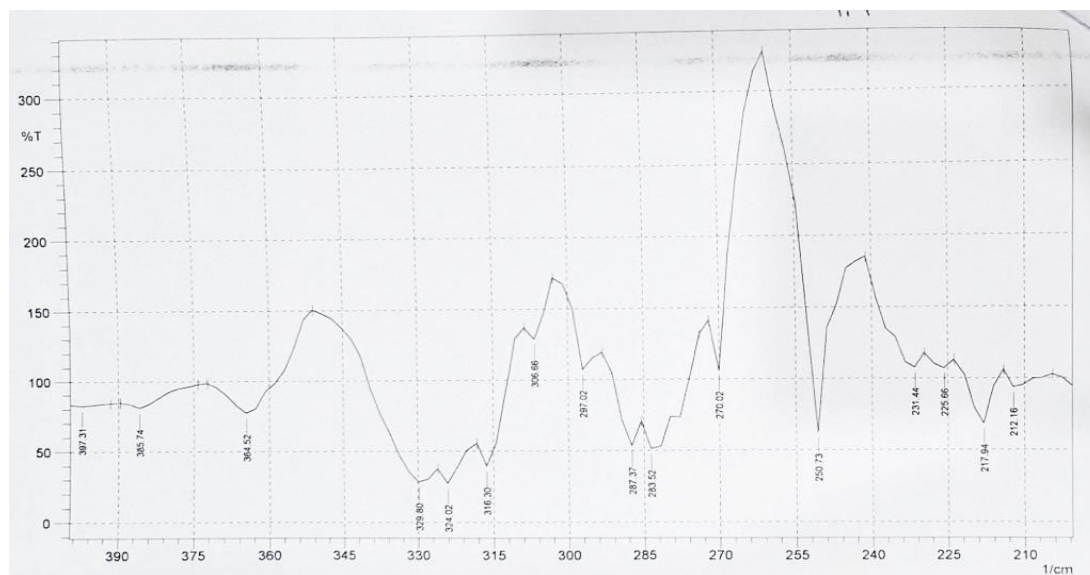


Figure 10 (b). FT-IR spectrum of Pd-L

Table 4. FT-IR spectral data of ligand (HL) and its complexes

Compounds	(H ₂ O) aqua	(NH)	Arom. proton	Aliph. proton	(N=N)	(sulfate)	C-O	M-N (M-O)
C ₁₉ H ₁₅ N ₅ O ₄ S	-	3381	3091	2977	1448	1160	1086	364
HL					1403	1086		(287)
[Pd(L)(H ₂ O)Cl]	3507	3385	3056	2978	1480	1145	1084	370
Square planer	1604				1390	1084		(280)
[Mn(L)Cl(H ₂ O) ₂]	3490	3382	3073	2979	1388	1164	1075	372
Tetrahedral	1602					1086		(283)
[Ni(L)(H ₂ O)Cl]	3506	3380	3134	2980	1469	1165	1079	361
Tetrahedral	1610				1369	1088		(278)

6. Study of Thermogravimetric Analysis for Compounds:

Pyrolysis studies for the ligand and some of its complexes were carried out depending on thermogravimetric analysis curve (TGA) by measuring the changes in masses of the substances under study relative to temperature when these substances obey controlled thermal program in a specific time. The result curve is considered as thermogravimetric curve, which indicates thermal stability, reaction rates, chemical structure and the thermal stability of the products as denoted in Table 6 in addition to each pyrolysis step occurred. DSC differential scanning calorimetry technique, defined as pyrolysis technique, was employed for estimating the amount of absorbed and released heat and for the thermal changes that happened for tested substance. Table 7, shows $T_i/^\circ\text{C}$, $T_f/^\circ\text{C}$, heat amount (ΔH) in J/g unit if it was exothermic or endothermic. TGA technique demonstrates that, the ligand (HL) is analyzed in three steps as illustrated in Fig. 11 that displays the mechanism of its degradation, the critical temperature at which the maximal transformation of ligand occurs and the

percentage of theoretical and calculated mass loss. It was found that, the estimated mass loss is 92.5393 % and the remnant is 7.4607 % whereas the calculated mass loss is 94.0353 % and the remnant is 5.9647 %.²⁹ Figure 12 of [Pt(L)(H₂O)Cl₃] complex, displays four steps degradation of the complex, the critical temperature at which the maximum mutation of complex is carried out and the percentage of theoretical is 30.2886 % and the remnant is 69.7114 %, and calculated mass loss 29.04 % and the remnant is 70.96 % as PtO.³⁰ And about [Mn(L)Cl(H₂O)₂] in Fig. 13, by the same approach we can investigate two pyrolysis steps ends with 14.3013 % and 13.7999 % as MnO which are the values of estimated and calculated remnants respectively.^{31,32} In addition to 85.6987 % and 86.2001% which are the values of estimated and calculated mass loss respectively. By the same way, we can also determine the pyrolysis steps of [Ni(L)(H₂O)Cl] complex that mentioned in Fig. 14 and in Table 5 and 6. Scheme 6, clearly explains the pyrolysis steps of the ligand and complexes.

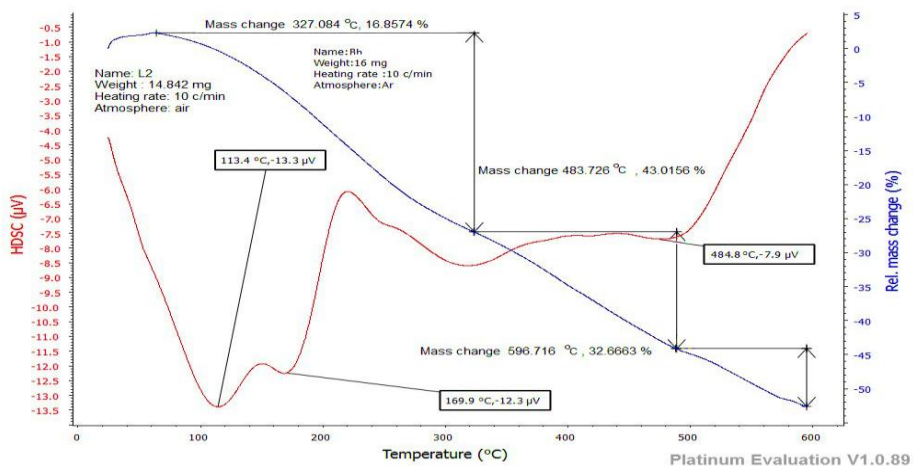


Figure 11. Pyrolysis sketch of ligand (HL)

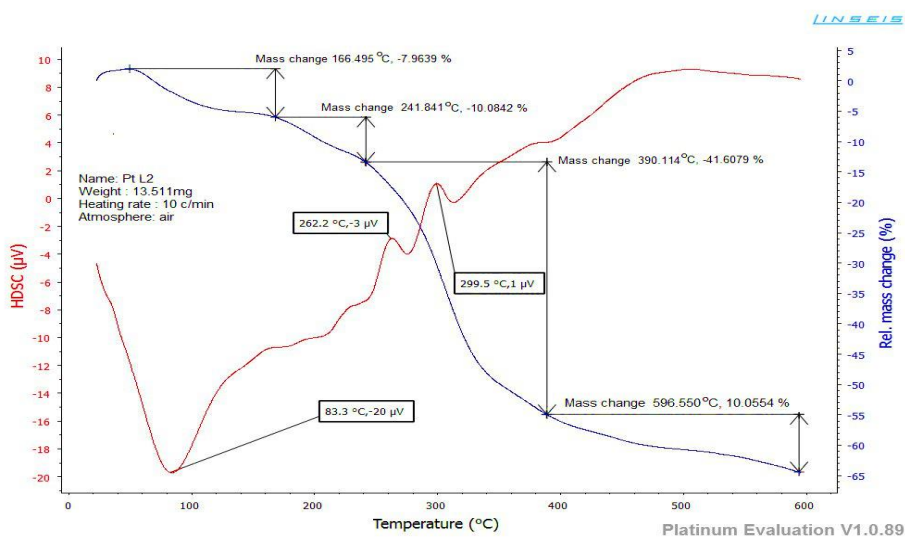


Figure 12. Pyrolysis sketch of Pt-L

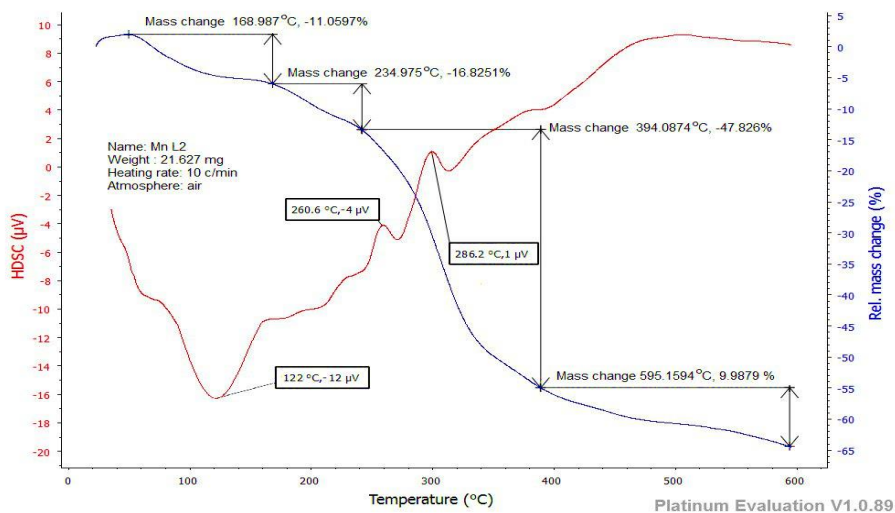


Figure 13. Pyrolysis sketch of Mn-L

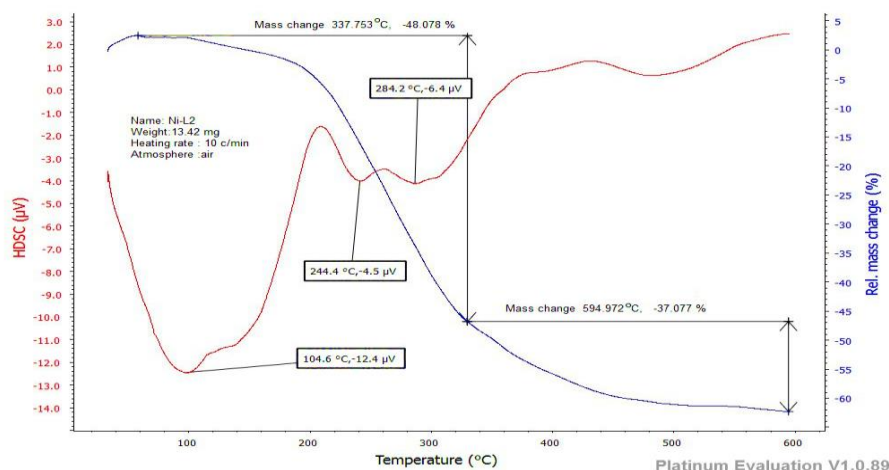
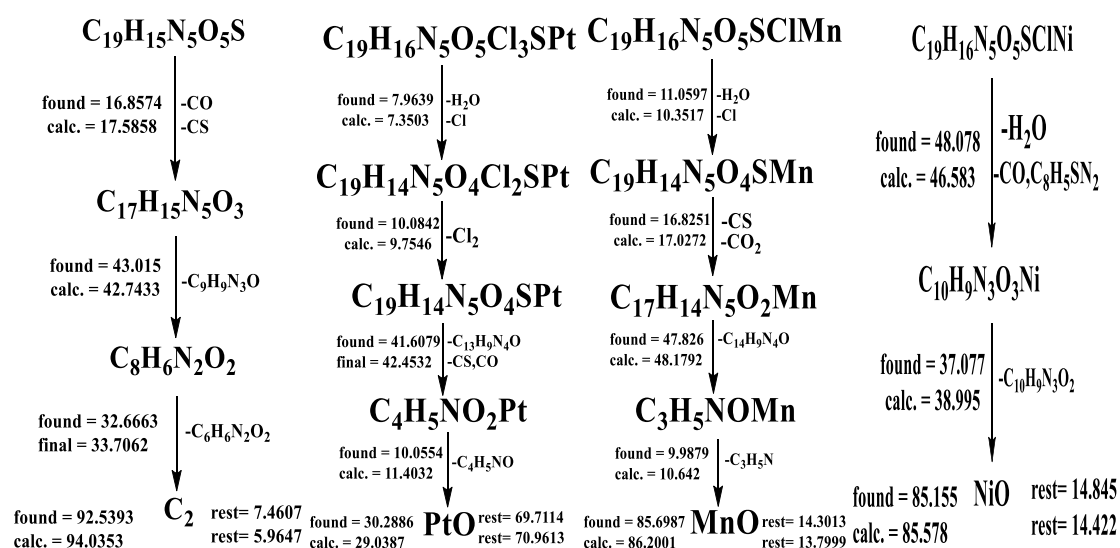


Figure 14. Pyrolysis sketch of Ni-L



Scheme 6. Tentative decomposition reaction of complexes

Table 5. TGA data of the ligand L and complexes

Compound	T _i / °C	T _f / °C	T _{DTG} max	% Estimated (calc.)		Assignment
				Mass loss	Total mass loss	
C ₁₉ H ₁₅ N ₅ O ₄ S HL	85	327.084	200	16.8574 (17.5858)	92.52 (94.02)	-CO -CS
	327.084	483.726	401	43.0156 (42.7433)		-C ₉ H ₉ N ₃ O
	483.726	596.716	541	32.6663 (33.7062)		-C ₆ H ₆ N ₂ O ₂
				C ₂		
Calculated: 94.0353% final = 5.9647%; Estimated 92.5393% final = 7.4607%						
[Mn(L)(H ₂ O) ₂ Cl]	40	168.987	110	11.0597 (10.3517)	85.6987 (86.2001)	-H ₂ O -Cl
	168.987	234.975	198	16.8251 (17.0272)		-CO ₂ -CS
	234.975	394.087	310	47.826 (48.1792)		-C ₁₄ H ₉ N ₄ O
	394.087	595.1594	485	9.9879 (10.642)		C ₃ H ₅ N MnO
Calculated: 86.2001% final = 13.7999%; Estimated 85.6987% final = 14.3013%						
[Ni(L)(H ₂ O)Cl]	62	337.753	190	48.078 (46.583)		-H ₂ O, -Cl -CO, -C ₈ H ₅ SN ₂

	337.753	594.972	462	37.077 (38.995)	85.155 (85.578)	-C ₁₀ H ₉ N ₃ O ₂ -NiO
Calculated:	85.578% final =14.422%;Estimated 85.155% final =14.845%					
	58	166.495	106	7.9639 (7.3503)		-H ₂ O -Cl
	166.495	241.841	200	10.0842 (9.7546)		-Cl ₂
[Pt(L)H ₂ OCl]	241.841	390.114	320	41.6079 (42.4532)	69.71 (70.96)	-CS,CO C ₁₃ H ₉ N ₄ O
	390.114	596.550	490	10.0554 (11.4032)		C ₄ H ₅ NO PtO
Calculated:	70.9613% final =29.0387%;Estimated 69.7114% final =30.288%					

Table 6. DSC records of the ligand L and complexes

Compound	T _i / °C	T _f / °C	T _{DTG} max	ΔH J/g	Max temp. °C and Type
	85	327.084	200	-13.3	113.4 - endothermic
C ₁₉ H ₁₅ N ₅ O ₄ S	327.084	483.726	401	-12.3	169.9 - endothermic
L	483.726	596.716	541	-7.9	484.8 - endothermic
	40	168.987	110	-12	122- endothermic
[Mn(L)(H ₂ O) ₂ Cl]	168.987	234.975	198	- 4	260.6- endothermic
	234.975	394.087	310	1	286.2- endothermic
	394.087	595.1594	485		
	62	337.753	190	-12.4	104.6- endothermic
[Ni(L)(H ₂ O) Cl]	337.753	594.972	462	-4.5	244.4- endothermic
				-6.4	244.2- endothermic
	58	166.495	106	-20	83.8- endothermic
[Pt(L)H ₂ OCl]	166.495	241.841	200	-3	262.2- endothermic
	241.841	390.114	320	1	299.5- endothermic
	390.114	596.550	490		

6. Investigation of Antioxidant Activity

The DPPH method was used to investigate antioxidant activity of the ligand and its metal complexes. Gallic acid was employed as a phenol containing reference. To provide a series of standards, five normal solutions of different concentrations (0.2, 0.4, 0.6, 0.8, and 1 mmol. l-1) of 10 mmol were prepared. An amount of 1-liter solution of Gallic acid, using ethanol as a diluent. 6 mL of 45 g of DPPH solution was added to 100 μL of each of normal Gallic acid solution. After 30 minutes of incubation at room temperature in the dark, the absorbance of the reaction mixture was measured using a UV-vis spectrophotometer at 517 nm. The following equation was used to calculate

percentage of root scavenger DPPH. Because of its simplicity and reliability, the majority of studies to evaluate the antioxidant activity of their targets uses the DPPH test, and Table 5 introduces the incomes of the radical scavenging activity of DPPH compounds. A lower IC₅₀ value refers to higher DPPH radical scavenging activity and according to the IC₅₀ values the order of oxidation activity is followed as (GA> [Pd(L)(H₂O)Cl]> [Ni(L)(H₂O)Cl]> [Mn(L)Cl (H₂O)₂]> [Pt(L)(H₂O)Cl]> L). The table showed that almost all of the compounds had radical scavenging activities in the DPPH assay. It was important to observe that azo complex showed better antioxidant activity than azo ligand³³⁻³⁶, as shown in Table 7.

Table 7. Antioxidant activity of Azo dye and its complexes

Compounds	Mean	Standard deviation	Coefficient of variation %	Correlation coefficient	IC ₅₀ (M) DPPH
GA	93.5600	2.0846	2.2281	0.9966	-6.0304
C ₁₉ H ₁₅ N ₅ O ₄ S (L)	45.7600	3.0663	3.3521	0.7632	1.6701
[Mn(L)Cl (H ₂ O) ₂]	38.8316	5.7753	4.1123	0.8816	0.6161
[Pd(L)(H ₂ O)Cl]	18.2735	3.6742	13.8665	0.7673	-1.3001
[Pt(L)(H ₂ O)Cl]	51.2276	4.7796	13.8221	0.7721	0.9681
[Ni(L)(H ₂ O)Cl]	50.3162	2.5007	3.7986	0.3387	0.3605

Conclusion:

Diazotization reaction in acidic media was carried out successfully in preparing a totally new azo-ligand 4-((2-hydroxyquinolin-7-yl)diazenyl)-N-(4-methylisoxazol-3-yl)benzenesulfonamide using Sulfamethoxazole and 2-hydroxyquinoline which in turn reacts with each of the next metal salts ; (Pt^{4+} , Pd^{2+} , Ni^{2+} and Mn^{2+}), in [1M:1L] molar ratio. The ligand and its complexes were identified using (1H and ^{13}C)-NMR, FT-IR, Uv-Vis, TGA, DSC and mass spectroscopic techniques. These techniques proved the suggested geometries of complexes , bidentate behavior of ligand and its bind positions depending on; the modifications that occurred in absorption bands (in FT-IR spectra) of some complexes compared to those that found in free ligand in addition to the spectral information obtained from other employed techniques. The estimated values and the elemental microanalysis results were found to be in good agreement with the theoretically calculated values. According to multinuclear NMR data, complexation occurs via the -NO moiety.

Authors' Declaration:

- Conflicts of Interest: None.
- We hereby confirm that all the Figures and Tables in the manuscript are mine ours. Besides, the Figures and images, which are not mine ours, have been given the permission for re-publication attached with the manuscript.
- Ethical Clearance: The project was approved by the local ethical committee in AL-Israa-University-College.

Authors' Contributions Statement:

A. G. A. conducted the practical side of the research, analysis of the results, and the writing of the manuscript. A. A. S. conceived the idea of the research, contributed in the analysis of the results and did the revision and the proofreading of the manuscript.

References:

1. Al-Daffay RK, Al-Hamdani AA. Synthesis, Characterization, and Thermal Analysis of a New Acidicazo Ligand's Metal Complexes. *Baghdad Sci. J.* 2022;19(3):121-33. <http://dx.doi.org/10.21123/bsj.2022.6709>
2. Kakanejadifard A, Esna-ashari F, Hashemi P, Zabardasti A. Synthesis and characterization of an azo dibenzoic acid Schiff base and its Ni (II), Pb (II), Zn (II) and Cd (II) complexes. *Spectrochimica Acta Part A: SAA.* 2013 Apr 1;106:80-5. <https://doi.org/10.1016/j.saa.2012.12.044>
3. Benkhaya S, M'rabet S, El Harfi A. Classifications, properties, recent synthesis and applications of azo dyes. *Heliyon.* 2020 Jan 1;6(1):e03271. <https://doi.org/10.1016/j.heliyon.2020.e03271>
4. Ghanavatkar CW, Mishra VR, Mali SN, Chaudhari HK, Sekar N. Synthesis, bioactivities, DFT and in-silico appraisal of azo clubbed benzothiazole derivatives. *J. Mol. Struct.* 2019 Sep 15;1192:162-71. <https://doi.org/10.1016/j.molstruc.2019.04.123>
5. Maliyappa MR, Keshavayya J, Mallikarjuna NM, Krishna PM, Shivakumara N, Sandeep T, Sailaja K, Nazrulla MA. Synthesis, characterization, pharmacological and computational studies of 4, 5, 6, 7-tetrahydro-1, 3-benzothiazole incorporated azo dyes. *J. Mol. Struct.* 2019 Mar 5; 1179:630-41. <https://doi.org/10.1016/j.molstruc.2018.11.041>
6. Feng J, Zhang S, Shi W, Zhang Y. Activity of sulfa drugs and their combinations against stationary phase *B. burgdorferi* in vitro. *J. Antibiot.* 2017;6(1):10. <https://doi.org/10.3390/antibiotics6010010>
7. Das D, Sahu N, Mondal S, Roy S, Dutta P, Gupta S, Sinha C. Structures, antimicrobial activity, DNA interaction and molecular docking studies of sulfamethoxazolyl-azo-acetylacetone and its nickel (II) complex. *Polyhedron.* 2015; 99: 77-86. <https://doi.org/10.1016/j.poly.2015.06.027>
8. Winum JY, Maresca A, Carta F, Scozzafava A, Supuran CT. Polypharmacology of sulfonamides: pazopanib, a multitargeted receptor tyrosine kinase inhibitor in clinical use, potently inhibits several mammalian carbonic anhydrases. *ChemComm.* 2012; 48(66):8177-8179. <https://doi.org/10.1039/C2CC33415A>
9. Khan DA, Knowles SR, Shear NH. Sulfonamide hypersensitivity: fact and fiction. *JACI: In Practice.* 2019; 7(7): 2116-2123. <https://doi.org/10.1016/j.jaip.2019.05.034>
10. Dorn JM, Alpern M, McNulty C, Volcheck GW. Sulfonamide drug allergy. *Curr. Allergy Asthma Rep.* 2018;18(7): 1-10. <https://doi.org/10.1007/s11882-018-0791-9>
11. Tailor A, Waddington JC, Hamlett J, Maggs J, Kafu L, Farrell J, et al. Definition of haptens derived from sulfamethoxazole: in vitro and in vivo. *Chem. Res. Toxicol.* 2019; 32(10): 2095-2106. <https://doi.org/10.1021/acs.chemrestox.9b00282>
12. Al-Fahemi JH, Khedr AM, Althagafi I, El-Metwaly NM, Saad FA, Katouah HA. Green synthesis approach for novel benzenesulfonamide nanometer complexes with elaborated spectral, theoretical and biological treatments. *Appl. Organomet. Chem.* 2018;32(9): e4460. <https://doi.org/10.1002/aoc.4460>
13. Adnan S. Synthesis, Spectral Characterization and Anticancer Studies of Novel Azo Schiff Base And its Complexes with Ag (I), Au (III) And Pt (IV) ions. *Egypt. J. Chem.* 2020 Dec 1;63(12):4749-56. [10.21608/EJCHEM.2020.23312.2438](https://doi.org/10.21608/EJCHEM.2020.23312.2438)
14. Chohan ZH, Shad HA. Sulfonamide-derived compounds and their transition metal complexes: synthesis, biological evaluation and X-ray structure of 4-bromo-2-[(E)-{4-[(3, 4-dimethylisoxazol-5 yl) sulfamoyl] phenyl} iminiomethyl] phenolate. *Appl. Organomet. Chem.* 2011; 25(8): 591-600. <https://doi.org/10.1002/aoc.1807>

15. Saad FA, El-Ghamry HA, Kassem MA, Khedr AM. Nano-synthesis, Biological Efficiency and DNA binding affinity of new homo-binuclear metal complexes with sulfa azo dye based ligand for further pharmaceutical applications. *J Inorg Organomet Polym Mater.* 2019; 29(4): 1337-1348. <https://doi.org/10.1007/s10904-019-01098-z>
16. Eugene-Osoikhia TT, Aleem AO, Ayeni F. Synthesis, characterisation and antimicrobial studies of mixed ligands Metal (II) complexes of sulfamethoxazole and N, N-Donors heterocycles. *Fudma J. Sci.* 2020;4(2): 217-232. <https://doi.org/10.33003/fjs-2020-0402-179>
- 17- Hadi MA, Kareem IK. synthesis, Characterization and Spectral Studies of a new Azo-Schiff base Ligand Derived from 3, 4-diamino benzophenone and its Complexes with Selected Metal Ions. *Research J. Adv. Sci.* 2020 Jul 2;1(1). <https://royalliteglobal.com/rjas/article/view/251>
18. Al-Majidi SM, Al-Khuzai MG. Synthesis and Characterization of New Azo Compounds Linked to 1, 8-Naphthalimide and Studying Their Ability as Acid-Base Indicators. *Iraqi J. Sci.* 2019 Nov 27:2341-52. <https://doi.org/10.24996/ijs.2019.60.11.4>
19. Al Zoubi W, Vian YJ, Veyan TS, Al-Hamdani A A S, Suzan Duraid Ahmed, Yang Gon Kim et al. Synthesis and bioactivity studies of novel Schiff bases and their complexes. *J. Phys. Org. Chem.* 2019; e4004: 1-7. <https://doi.org/10.1002/poc.4004>
20. Moamen SR, Altalhi T, Safyah BB, Ghaferah HA, Kehkashan A. New Cr(III), Mn(II), Fe(III), Co(II), Ni(II), Zn(II), Cd(II), and Hg(II) Gibberellate Complexes: Synthesis, Structure, and Inhibitory Activity Against COVID-19 Protease. *Russ. J. Gen. Chem.* 2021; 91(5): 890–896. <https://doi.org/10.1134/S1070363221050194>
21. Kadhim SM, Mahdi SM. Preparation and Characterization of New (Halogenated Azo-Schiff) Ligands with Some of their Transition Metal Ions Complexes. *Iraqi J. Sci.* 2022 Aug 31:3283-99. <https://doi.org/10.24996/ijs.2022.63.8.4>
22. Abd Wannas F, Azooz EA, Ridha RK, Jawad SK. Separation and micro determination of zinc (II) and cadmium (II) in food samples using cloud point extraction method. *Iraqi J. Sci.* 2023 Feb 28:1049-61. <https://doi.org/10.24996/ijs.2023.64.3.2>
23. Almáši M, Vilková M, Bednarčík J. Synthesis, characterization and spectral properties of novel azo-azomethine-tetracarboxylic Schiff base ligand and its Co (II), Ni (II), Cu (II) and Pd (II) complexes. *Inorganica Chim. Acta.* 2021 Jan 24;515:120064. <https://doi.org/10.1016/j.ica.2020.120064>
24. Salem OM, Abdelsalam A, Boroujerdi A. Bioremediation potential of *Chlorella vulgaris* and *Nostoc paludosum* on azo dyes with analysis of metabolite changes. *Baghdad Sci J.* 2021 Sep 1;18(3):445-54. <http://dx.doi.org/10.21123/bsj.2021.18.3.0445>
25. Kareem IK, Hadi MA. Synthesis and characterization of some transition metal complexes with new azo-schiff base ligand 3, 4-bis (((1E, 2E)-2-((2-(4-(Z)-(3-Hydroxyphenyl) Diazenyl) Naphthalen-1-yl) amino) ethyl) imino)-1, 2-Diphenylethylidene) Amino Phenyl(phenyl) Methanone. *Egypt. J. Chem.* 2020 Jan 1;63(1):301-13. <https://doi.org/10.21608/ejchem.2019.18924.2166>
26. Ameer HA, Hussain AF. Spectrophotometric Determination of Micro Amount of Chromium (III) Using Sodium 4-((4, 5-diphenyl-imidazol-2-yl) diazenyl)-3-hydroxynaphthalene-1-sulfonate in the Presence of Surfactant, Study of Thermodynamic Functions and Their Analytical Applications. *Baghdad Sci. J.* 2023. <https://doi.org/10.21123/bsj.2023.7393>
27. Anitha C, Sheela CD, Tharmaraj P, Sumathi S. Spectroscopic studies and biological evaluation of some transition metal complexes of azo Schiff-base ligand derived from (1-phenyl-2, 3-dimethyl-4-aminopyrazol-5-one) and 5-((4-chlorophenyl) diazenyl)-2-hydroxybenzaldehyde. *Spectrochimica Acta Part A: SAA.* 2012 Oct 1;96:493-500. <https://doi.org/10.1016/j.saa.2012.05.053>
28. Kareem MJ, Al-Hamdani AAS, Ko YG, Al Zoubi W, Mohammed SG. Synthesis, characterization, and determination antioxidant activities for new Schiff base complexes derived from 2-(1H-indol-3-yl)-ethylamine and metal ion complexes. *J Mol Struct.* 2021; 1231(5): 1-30. <https://doi.org/10.1016/j.molstruc.2020.129669>
29. Kareem MJ, Al-Hamdani AAS, Jirjees VY, Khan ME, Allaf AW, Al Zoubi W, Preparation, spectroscopic study of Schiff base derived from dopamine and metal Ni (II), Pd (II), and Pt (IV) complexes, and activity determination as antioxidants. *J Phys Org Chem.* 2020; 34(3): 1-15. <https://doi.org/10.1002/poc.4156>
30. Reda SM, Al-Hamdani AA. Mn (II), Fe (III), Co (II) and Rh (III) complexes with azo ligand: Synthesis, characterization, thermal analysis and bioactivity. *Baghdad Sci. J.* 2022. <https://doi.org/10.21123/bsj.2022.7289>
31. Al-Hamdani AAS, Hamoodah RG. Transition metal complexes with tridentate ligand: preparation, spectroscopic characterization, thermal analysis and structural studies. *Baghdad sci j.* 2016; 13(4): 770-781. <http://dx.doi.org/10.21123/bsj.2016.13.4.0770>
32. Deghadi RG, Mahmoud WH, Mohamed GG. Metal complexes of tetradentate azo-dye ligand derived from 4, 4'-oxydianiline: Preparation, structural investigation, biological evaluation and MOE studies. *Appl. Organomet. Chem.* 2020 Oct;34(10):e5883. <https://doi.org/10.1002/aoc.5883>
33. Al-Muhanaa SS, Al-Khafagy AH. Preparation and Biological Activities of New Heterocyclic Azo Ligand and Some of Its Chelate Complexes. *Nano Biomed. Eng.* 2018 Mar 1;10(1):46-55. <https://doi.org/10.5101/nbe.v10i1.p46-55>
34. Aziz KA, Yousif TY. Characterization Studies on Mn (II), Co (II), Ni (II), Cu (II), Zn (II) and Cd (II) Complexes with New Ligands Derived from Anthraquinone Substance. *Iraqi J. Sci.* 2022 Jul 31:2804-13. <https://doi.org/10.24996/ijs.2022.63.7.5>
35. Venugopal N, Krishnamurthy G, Bhojyanaik HS, Krishna PM. Synthesis, spectral characterization and biological studies of Cu (II), Co (II) and Ni (II)

complexes of azo dye ligand containing 4-amino antipyrine moiety. J. Mol. Struct. 2019 May 5;1183:37-51.

<https://doi.org/10.1016/j.molstruc.2019.01.031>

36. Mallikarjuna NM, Keshavayya J, Maliyappa MR, Ali RS, Venkatesh T. Synthesis, characterization, thermal

and biological evaluation of Cu (II), Co (II) and Ni (II) complexes of azo dye ligand containing sulfamethaxazole moiety. J. Mol. Struct. 2018 Aug 5;1165:28-36.

<https://doi.org/10.1016/j.molstruc.2018.03.094>

تحضير و تشخيص و دراسة التحلل الحراري و النشاط المضاد للاكسدة لبعض ايونات المعقدات المعدنية amino-N-(5--و quinolin-2-ol مع ليكاند ازو جديد مشتق من $(Ni^{2+}, Pt^{4+}, Pd^{2+}, \text{ and } Mn^{2+})$ methylisoxazol-3-yl)benzenesulfonamide

عباس علي صالح الحمداني²

عذراء غازي عبد الرزاق¹

¹ قسم تقنيات الاجهزة الطبية، كلية الاسراء الجامعة، بغداد، العراق

² قسم الكيمياء، كلية العلوم للبنات، جامعة بغداد، بغداد، العراق

الخلاصة :

تم إجراء تفاعل الازوتة بين الكينولين-2-ol و (2-كلورو-1-4) - (5-methylisoxazol-3-yl) sulfamoyl phenyl) - (Mn⁺² و Ni⁺²، Pt⁺⁴، Pd⁺²، +) ligand-HL ، وهذا بدوره يتفاعل مع أيونات الفلزات التالية (Ni⁺²، Pt⁺⁴، Pd⁺²، +) لتشكيل معقدات مستقرة ذات أشكال هندسية فريدة مثل (رباعي السطوح لكل من Ni⁺² و Mn⁺²، ثماني السطوح لـ Pd⁺² و مربع مستوي لـ Pd⁺²). تم الكشف عن المعقدات عن طريق استخدام وسائل طيفية تشمل الأشعة فوق البنفسجية التي أثبتت الأشكال الهندسية التي تم الحصول عليها، وأثبت نقل فوربييه تكوين مجموعة الأزو والتنسيق مع أيون المعدن من خلالها، أثبتت دراسات الانحلال الحراري (TGA & DSC) تنسيق بقايا الماء مع أيونات المعادن داخل مجال التناسق وكذلك ذرات الكلور. علاوة على ذلك، فإن التحليل الجزئي للعناصر و AAS الذي أعطى النتيجة المقابلة مع النتائج النظرية. أيون. تم تقييم الأنشطة المضادة للاكسدة لهذه المركبات ضد جذري (DPPH) وتمت مقارنتها بمضادات الأكسدة الطبيعية القياسية، حمض الأسكوربيك. تظهر النتائج أن هذه المركبات تظهر أنشطة ممتازة في إزالة الجذور

الكلمات المفتاحية: مضادات الاكسدة، صبغة الازو، مطيافية الكتلة، سلفاميثاكسازول، التحلل الحراري.